

TRACK RECONSTRUCTION AND ALIGNMENT WITH THE CMS SILICON TRACKER

F.-P. SCHILLING (CMS COLLABORATION)

Physics Department, CERN, CH-1211 Geneva 23, Switzerland

E-mail: frank-peter.schilling@cern.ch

This report presents recent results on track reconstruction and alignment with the silicon tracker of the CMS experiment at the LHC, obtained with a full detector simulation. After an overview of the layout of the tracker and its material budget, the baseline algorithm for track reconstruction is discussed. The performance of the track reconstruction and its dependence on misalignment is shown. The concept for alignment of the CMS tracker, using a laser alignment system as well as three different track-based alignment algorithms, is presented.

1. INTRODUCTION

This report^a presents recent results¹ on track reconstruction and alignment with the silicon tracker of the CMS experiment at the LHC, obtained with a full detector simulation. After an overview of the layout of the tracker and its material budget, the baseline algorithm for track reconstruction is discussed. The performance of the track reconstruction and its dependence on misalignment is shown. The concept for alignment of the CMS tracker, using a laser alignment system as well as three different track-based alignment algorithms, is presented.

2. THE CMS SILICON TRACKER

The CMS Silicon Tracker (Figure 1) is one of the main components of the CMS experiment at the LHC. It consists of ~ 15000 silicon strip and pixel sensors covering an active area of $\sim 200 \text{ m}^2$ within the tracker volume of 24.4 m^3 . The full tracker has a radius of $\sim 110 \text{ cm}$ and covers pseudorapidity values up to $\eta = 2.4$.

The Barrel strip detector consists of 4 inner (TIB) and 6 outer (TOB) layers (Figure 2). The first two layers in TIB and

TOB use double-sided sensors. The Endcap strip detector is made of 3 inner (TID) and 9 outer (TEC) disks (rings 1,2 and 5 are double sided). The Pixel detector consists of 3 barrel layers at $r = 4.4, 7.3$ and 10.2 cm , and of two endcap disks.

The Strip Sensors consist of 512 or 768 strips with a pitch of $80 \dots 200 \mu\text{m}$. Their resolution in the precise coordinate is in the range $20 \dots 50 \mu\text{m}$. The Pixel sensors are made of pixels of size $100(r\phi) \times 150(z) \mu\text{m}^2$ with a resolution of $10 \dots 15 \mu\text{m}$. The modules are mounted on carbon-fiber structures and housed inside a temperature controlled outer support tube. The operating temperature will be around -20°C . Figure 3 shows two recent photographs from the integration of tracker components.

3. TRACKER MATERIAL BUDGET

The CMS tracker includes both sensitive volumes and non-sensitive ones. Since the tracker requires a large amount of low-voltage power, a large amount of heat needs to be dissipated. Therefore, a large fraction of the tracker material consists of electrical cables and cooling services. Other non-sensitive parts include support structures, electronics, the beam-pipe, and the thermal screen outside the tracker.

^aPoster presented at ICHEP 2006, Moscow

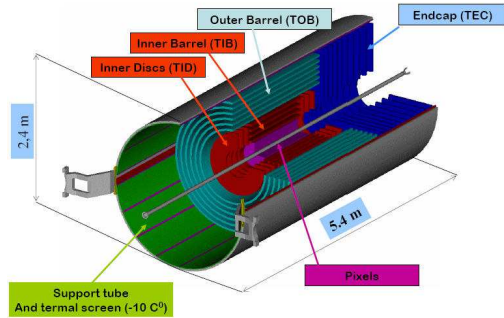


Fig. 1. Illustration of the CMS tracker. The various components such as barrel and endcap strip and pixel detectors, are housed in a support tube 2.4 m in diameter and 5.4 m in length.

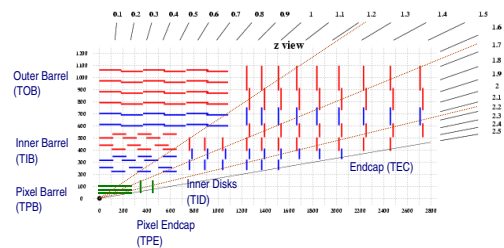


Fig. 2. Illustration of the CMS tracker layers, showing one quarter of the full tracker in rz view.

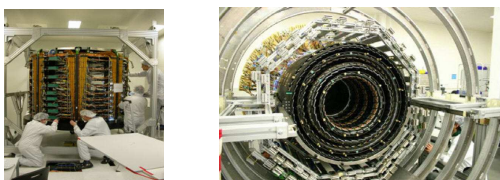


Fig. 3. Photographs from the integration of tracker components. Left: TEC Integration; Right: One half of TIB/TID completed.

As a result, the tracker material budget can exceed the equivalent of one radiation length for certain regions of η , which affects hadron and electron reconstruction. The decomposition of the tracker material in terms of radiation lengths and interaction lengths versus η for the different subdetectors is shown in Figure 4.

4. TRACK RECONSTRUCTION

Track reconstruction in a dense environment needs an efficient search for hits during the pattern recognition stage and a fast propagation of trajectory candidates. In the CMS tracker, these tasks benefit from the arrangement of the sensitive modules in practically hermetic layers as well as from the almost constant four Tesla magnetic field provided by the CMS solenoid magnet. Since the typical step length for the propagation of track parameters is of the order of the distance between two layers, a helical track model is adequate.

For reconstruction purposes the detailed distribution of passive material as used in the simulation is replaced by an attribution of material to layers. This model simplifies the estimation of energy loss and multiple scattering, which can be done at the position of the sensitive elements without additional propagation steps.

The baseline algorithm for track reconstruction ² in CMS is the Combinatorial Kalman Filter. After the tracker hits have been reconstructed (clustering and position estimation), track reconstruction proceeds through the following four stages:

- Trajectory Seeding
- Pattern Recognition
- Trajectory Cleaning
- Track fitting and smoothing

In the following subsections, these steps are explained in more detail.

4.1. Trajectory Seeding

Seed generation provides initial trajectory candidates for the full track reconstruction. A seed must define initial trajectory parameters and errors. Hence, five parameters are needed to start trajectory building. Therefore, the standard trajectory seeds in the CMS tracker are constructed from pairs of

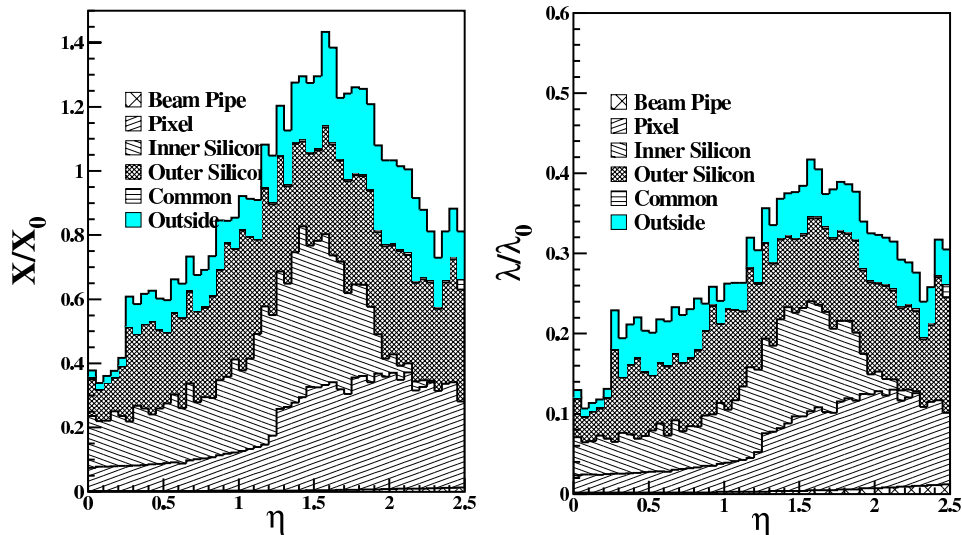


Fig. 4. Tracker material budget in units of radiation length (left) and interaction length (right) as a function of η for the different subunits.

hits in the pixel detector and a vertex constraint. The pixel detector is well suited for seeding due to its low occupancy, its proximity to the beam spot and due to the 2D measurement capability in both $r\phi$ and rz . The seed finding efficiency is $> 99\%$.

Alternatively to the baseline seeding, a seeding using the innermost layers of the strip tracker has also been implemented, to be used for example at the start-up when the pixel detector will not yet be installed. In addition, external seeds provided by the calorimeter or the muon detector can be used.

4.2. Pattern Recognition

Trajectory building is based on a combinatorial Kalman filter method. The filter proceeds iteratively from the seed layer, starting from a coarse estimate of the track parameters provided by the seed, and including the information of the successive detection layers one by one. With each included layer, the track parameters are better constrained. In the extrapolation of the trajectory from layer to layer, the effects of energy loss and

multiple scattering are accounted for.

Trajectory candidates are added for each compatible hit (including an additional trajectory without a measured hit in order to account for inefficiencies), and the trajectory parameters are updated according to the Kalman filter formalism. The best trajectory candidates are grown in parallel up to the outermost layers.

4.3. Trajectory Cleaning

Ambiguities in track finding arise because a given track may be reconstructed starting from different seeds, or because a given seed may result in more than one trajectory candidate. These ambiguities must be resolved in order to avoid double counting of tracks.

The ambiguity resolution is based on the fraction of hits that are shared between two trajectories. It is applied twice: the first time on all trajectories resulting from a single seed, and the second time on the complete set of track candidates from all seeds.

4.4. Track fitting and smoothing

For each trajectory, the building stage results in a collection of hits and an estimate of the track parameters. However, the full information is only available at the last hit of the trajectory, and the estimate may be biased by constraints applied during the seeding stage. Therefore the trajectory is refitted using a least squares approach, implemented as a combination of a standard Kalman filter and smoother. While the filter runs inside-out, in the smoothing step a second filter is run outside-in. In both cases, the initial covariance matrix of the track parameters is scaled by a large factor to avoid possible biases. At each hit the updated parameters of the smoothing filter are combined with the predicted parameters of the first filter. The combination yields optimal estimates of the track parameters at the surface of each hit.

5. TRACKING PERFORMANCE

5.1. Track finding efficiency

The efficiency for reconstructing single tracks with the combinatorial Kalman filter has been estimated using samples of muons and pions with transverse momenta of 1, 10 and 100 GeV. The results are shown in Figure 5. Here, reconstructed tracks are required to have at least 8 hits and a minimum p_T of 0.8 GeV. A track is deemed to be successfully reconstructed if it shares more than 50% of the hits with a simulated track.

The global track finding efficiency for muons is excellent, exceeding 98% over most of the tracker acceptance. The drop of efficiency in the region $|\eta| < 0.1$ is due to the gaps between the sensors in the ladders of the pixel detector at $z = 0$. At high η , the drop in efficiency is mainly due to the lack of coverage by the two pairs of pixel endcap disks.

For hadrons, the efficiency is between 75 and 95%, depending on momentum and η .

It is lower compared with the efficiency for muons because the hadrons interact with the tracker material.

5.2. Resolution

Five parameters are chosen to describe a track: The transverse and longitudinal impact parameters d_0 and z_0 , the angular parameters ϕ and $\cot\theta$, and the transverse momentum p_T . The resolutions in d_0 and in p_T are shown in Figure 6.

At high momentum, the impact parameter resolution is fairly constant and is dominated by the hit resolution of the first hit in the pixel detector. At lower momenta, the d_0 resolution is progressively degraded by multiple scattering, until the latter becomes dominant.

The transverse momentum resolution is around 1...2% up to a pseudorapidity of $|\eta| < 1.6$ at high momentum. For higher values of $|\eta|$ the lever arm of the measurement is reduced. The degradation around $|\eta| = 1.0$ is due to the gap between the barrel and the endcap disks. At $p_T = 100$ GeV, the tracker material accounts for 20...30% of the transverse momentum resolution. At lower momenta, the resolution is dominated by multiple scattering and its distribution reflects the amount of material traversed by the track.

6. IMPACT OF MISALIGNMENT

The large number of independent silicon sensors and their excellent intrinsic resolution of 10...50 μm make the alignment of the CMS strip and pixel trackers a complex of challenging task. The residual alignment uncertainties should not lead to a significant degradation of the intrinsic tracker resolution. For example, to achieve a desired precision on the measurement of the W boson mass of 15...20 MeV, the momentum scale has to be known to an accuracy of 0.02 to 0.025%,

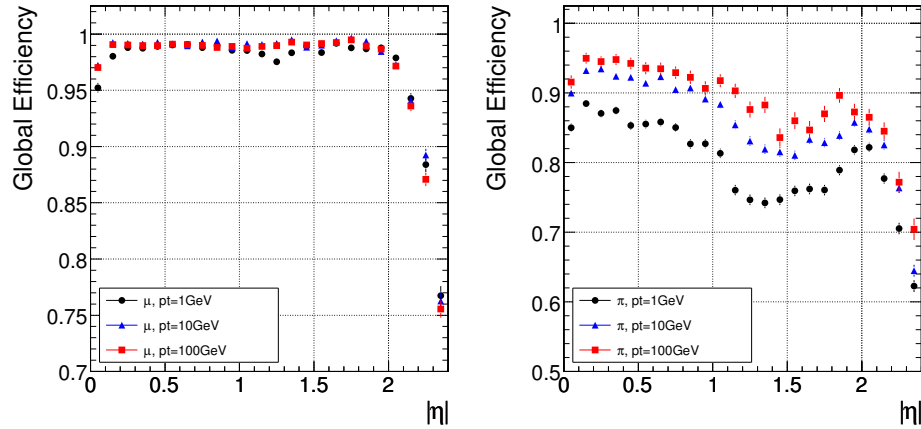


Fig. 5. Track finding efficiency for muons (left) and pions (right) with $p_T = 1, 10$ and 100 GeV as a function of η .

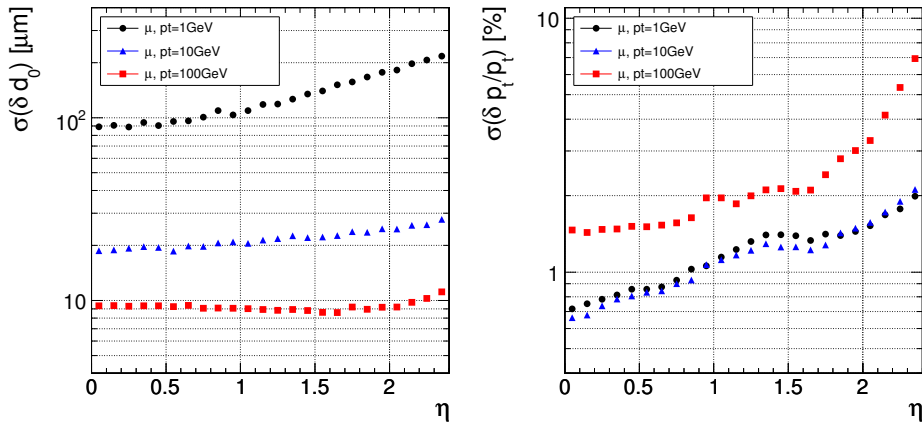


Fig. 6. Resolution in transverse impact parameter d_0 (left) and in p_T (right) for muons with $p_T = 1, 10$ and 100 GeV.

which implies the absolute detector positions to be known with a precision of better than $10 \mu\text{m}$ in the $r\phi$ plane. Misalignment will degrade the track parameter resolution and hence affect the physics performance of the tracker, for instance the mass resolution of resonances and b-tagging and vertexing performances.

In order to assess the impact of misalignment on the tracking and vertexing performance in general, but also in specific physics channels in particular, a realistic model of misalignment effects³ has been implemented

in the standard CMS software, where the displacement of detector modules is implemented at reconstruction level using a dedicated software tool which is able to move and rotate all tracker parts (individual sensors as well as composed structures such as whole layers or disks). In addition, the position error assigned to a reconstructed hit can be increased by adding an additional error that reflects the size of the assumed misalignment (alignment position error).

Two default *misalignment scenarios* have been implemented in the software:

	Pixel		Silicon Strip			
	Barrel	Endcap	Inner Barrel	Outer Barrel	Inner Disk	Endcap
First Data Taking Scenario						
Modules	13	2.5	200	100	100	50
Ladders/Rods/Rings/Petals	5	5	200	100	300	100
Long Term Scenario						
Modules	13	2.5	20	10	10	5
Ladders/Rods/Rings/Petals	5	5	20	10	30	10

- **First Data Taking Scenario:**

This scenario is supposed to resemble the expected conditions during the first data taking of CMS (few 100 pb^{-1} of accumulated luminosity). It assumes that the pixel detector has been aligned to a reasonable level using tracks. For the strip detector it is assumed that no track-based alignment is possible due to insufficient high p_T track statistics, so that only survey information is available. In addition, the LAS would provide constraints on the positions of the larger structures of the strip tracker.

- **Long Term Scenario:** It is assumed that after the first few fb^{-1} of data have been accumulated, a first complete track-based alignment down to the sensor level has been carried out, resulting in an overall alignment uncertainty of the strip tracker of $\sim 20 \mu\text{m}$.

The placement uncertainties used in the scenarios are listed in Table 1. As an illustration of the implementation and use of these misalignment scenarios, Figure 7 shows the effects of misalignment on track-finding efficiency and transverse momentum resolution for single muons ⁴. The track finding efficiency is close to unity for $|\eta| < 2$ for all misalignment scenarios, provided the alignment

position error is taken into account. If not, the efficiency is significantly reduced, which is illustrated in Figure 7 for the short term scenario. The dip in the distribution in the range $1.2 < |\eta| < 2.0$ is due to tracks passing through the TID, which has large alignment uncertainties due to the missing laser alignment system. For $|\eta| > 2.2$ the inclusion of the alignment position error does not improve the efficiency due to the large track extrapolation uncertainties involved in the very forward direction.

7. ALIGNMENT OF THE CMS TRACKER

The alignment strategy for the CMS tracker foresees that in addition to the knowledge of the positions of the modules from measurements at construction time, the alignment will proceed by two means: A Laser Alignment System (LAS) and track-based alignment.

7.1. Laser Alignment System

The Laser Alignment System uses infrared laser beams to monitor the positions of selected detector modules of the strip tracker and of special alignment sensors in the muon system. Therefore it operates globally on the larger tracker composite structures (TIB, TOB, TEC disks) and cannot determine the position of individual modules. The goal of the LAS is to provide alignment informa-

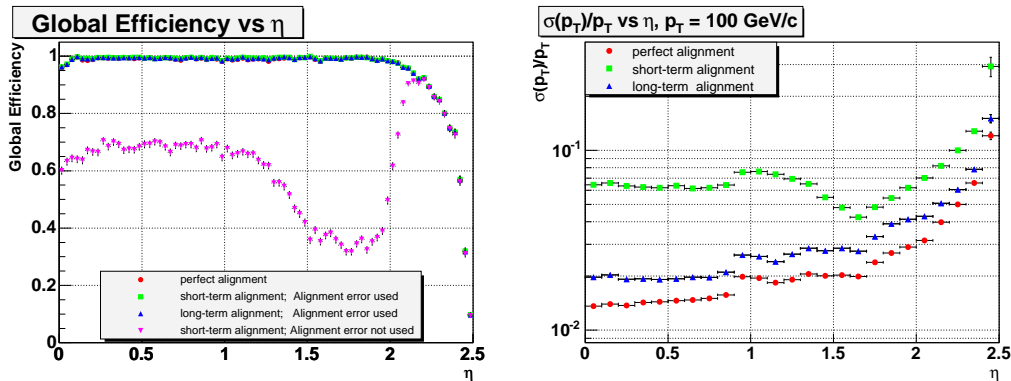


Fig. 7. Track finding efficiency (left) and p_T resolution vs η (right) for muons with $p_T = 100$ GeV. If the alignment uncertainty is not accounted for, the efficiency is significantly degraded. The p_T resolution deteriorates significantly with misalignment, in particular for the short-term scenario.

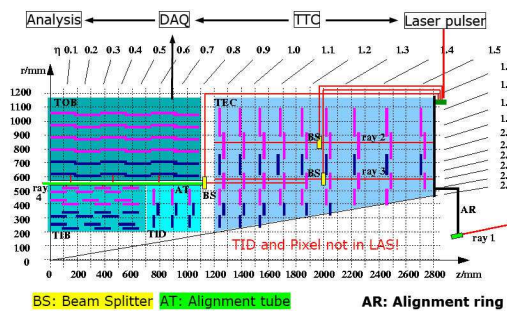


Fig. 8. Illustration of the CMS Laser Alignment System. The laser beams are distributed by beam splitters (BS) and alignment tubes (AT). The link to the muon system is implemented on the alignment rings (AR) that are connected to the tracker back disks.

tion on a continuous basis, providing position measurements of the tracker substructures at the level of $100 \mu\text{m}$, which is mandatory for pattern recognition and for the High Level Trigger. In addition possible structure movements can be monitored at the level of $10 \mu\text{m}$.

The LAS design is illustrated in Figure 8. Each tracker endcap (TEC) uses in total 16 beams distributed in ϕ and crossing all 9 TEC disks, which are used for the internal alignment of the TEC disks. The other 8 beams are foreseen to align TIB, TOB and TEC with respect to each other. Finally, there is a link to the muon system. As laser pulses are fired with a rate of around 100

Hz, a full snapshot of the tracker structure can be taken in a few seconds. The LAS is foreseen to operate both in dedicated runs and during physics data taking, so that the alignment can be monitored on a continuous basis.

7.2. Track Based Alignment

Track-based alignment was shown to be the optimal method for the alignment of large tracking detectors in previous experiments. However, it represents a major challenge at CMS because the number of degrees of freedom involved is very large: Considering 3+3 translational and rotational degrees of freedom for each of the ~ 15000 modules leads to $\mathcal{O}(100,000)$ alignment parameters, which have to be determined with a precision of $\sim 10 \mu\text{m}$. Moreover, the full covariance matrix is of size $\mathcal{O}(10^{10})$.

In CMS, three different track-based alignment algorithms are considered, some having been established at other experiments, others newly developed. In the following, the main features and initial results of using these algorithms in CMS are summarized.

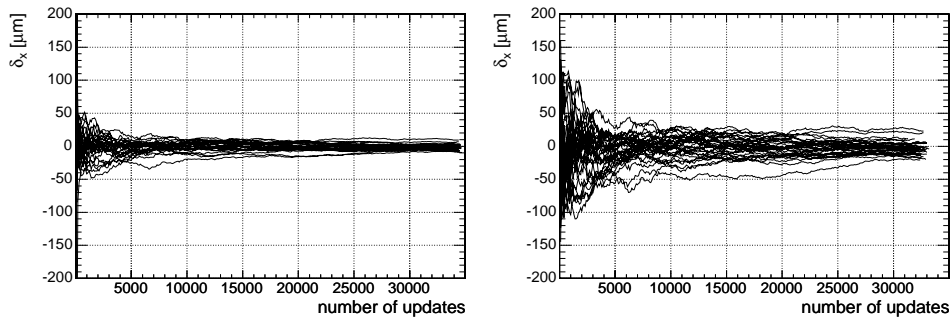


Fig. 9. Kalman Filter alignment: Residuals in local x for TIB layers 1 (left) and 2 (right) as a function of the number of processed tracks.

7.2.1. Kalman Filter

A method for global alignment using charged tracks can be derived from the Kalman filter. The method is iterative, so that the alignment parameters are updated after each track. It can be formulated in such a way that no large matrices have to be inverted⁵. In order to achieve a global alignment the update is not restricted to the detector elements that are crossed by the track, but can be extended to those elements that have significant correlations with the ones in the current track. This requires some bookkeeping, but keeps the computational load to an acceptable level. It is possible to use prior information about the alignment obtained from mechanical survey measurements as well as from laser alignment. The algorithm can also be extended to deal with kinematically constrained track pairs (originating from particle decays).

The algorithm has been implemented in the CMS software and studied in two small subsets of the silicon tracker: A telescope-like section of the inner and outer barrel, and a wheel-like subset of the inner barrel, consisting of 156 modules in 4 layers. The tracks used were simulated single muons with $p_T = 100$ GeV. Random misalignment with a standard deviation of $\sigma = 100 \mu\text{m}$ was applied to the local x and y positions of the modules. Results from the alignment of the

wheel-like setup are shown in Figure 9. It shows the evolution of the differences between true and estimated x -shifts for layers 1 and 2. A total of 100 000 tracks were processed. As can be seen, the speed of convergence depends on the layer. More results can be found in⁵.

7.2.2. Millepede-II

Millepede⁶ is a well established and robust program package for alignment which has been used successfully at other experiments, for example at H1, CDF, LHCb and others. Being a non-iterative method, it has been shown that it can improve the alignment precision considerably with respect to other algorithms.

Millepede is a linear least-squares algorithm which is fast, accurate and can take into account correlations among parameters. In the least-squares fit local track parameters and global alignment parameters are fitted simultaneously. The solution for the alignment parameters is obtained from a matrix equation for the global parameters only. For N alignment parameters this requires the inversion of a $N \times N$ matrix. However, this method can only be used up to $N \sim 10000$ due to CPU and memory constraints. The alignment of the CMS tracker exceeds this limit by one order of magnitude. Therefore, a new version Millepede-II⁷ was developed,

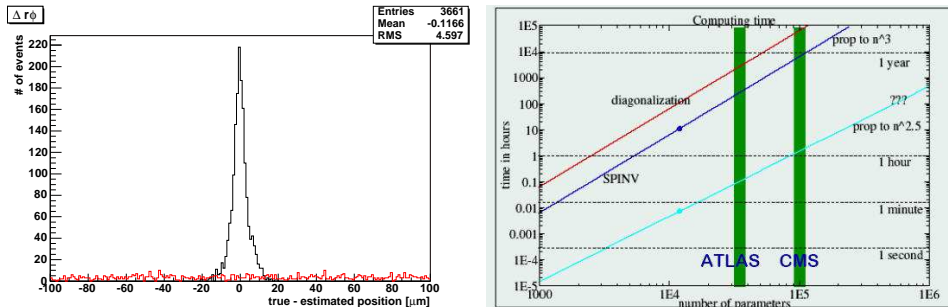


Fig. 10. Millepede-II: Left: Residuals in $r\phi$ in the strip tracker barrel before (red) and after (black) alignment using Millepede-II. Right: CPU time as a function of alignment parameters for matrix inversion (blue) and Millepede-II.

which offers different solution methods, and is applicable for N much larger than 10000. In Millepede-II, in addition to the matrix inversion and a diagonalization method, a new method for the solution of very large matrix equations is implemented. This minimum residual method applicable for sparse matrices determines a good solution by iteration in acceptable time even for large N .

Millepede-II has been interfaced to the CMS software and the alignment of parts of the CMS tracker has been carried out using different scenarios ⁷. As an example, Figure 10 (left) shows hit residuals in $r\phi$ for the new iterative method. Each individual sensor of the tracker was misaligned. The alignment procedure was carried out in the barrel region ($|\eta| < 0.9$) of the strip tracker using 1.8 million $Z^0 \rightarrow \mu^+\mu^-$ events. The pixel layers and the outermost barrel layer were kept fixed, resulting in ~ 8400 alignment parameters. The convergence is very good, and the results obtained are identical to those using the matrix inversion method, but the new method being faster by about three orders of magnitude.

Figure 10 (right) shows the needed CPU time as a function of the number of alignment parameters for the diagonalization and matrix inversion methods as well as for the new method used in Millepede-II. It can be seen that Millepede-II is expected to be ca-

pable to solve the full CMS tracker alignment problem within reasonable CPU time.

7.2.3. HIP Algorithm

An iterative alignment algorithm using the Hits and Impact Points (HIP) method was developed in ⁸. It is able to determine the alignment of individual sensors by minimizing a local χ^2 function depending on the alignment parameters, constructed from the track-hit residuals on the sensor. Correlations between different sensors are not explicitly included, but taken care of implicitly by iterating the method, which involves consecutive cycles of calculating the alignment parameters and refitting the tracks. The algorithm is computationally light because no inversion of large matrices is involved. An alternative implementation of the algorithm is designed to align composite detector structures for a common translation and rotation ⁹, for example pixel ladders or layers. The composite alignment involves only a small number of parameters, and therefore a rather small number of tracks is sufficient to carry out alignment already in the beginning of data taking.

The HIP algorithm has been used in ⁹ for the alignment of the pixel barrel modules using the First Data Taking misalignment scenario (see section 6). The pixel endcaps and the strip tracker are not misaligned. The

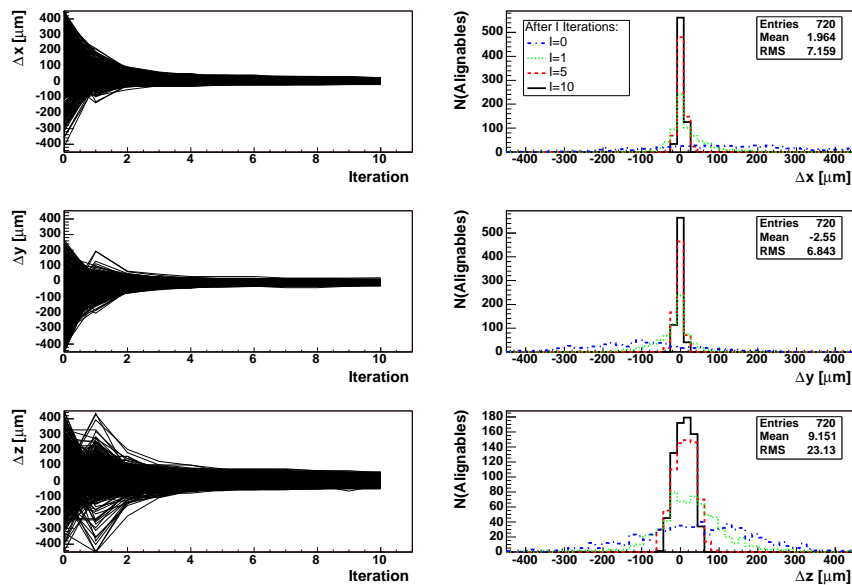


Fig. 11. Alignment of the Pixel barrel modules with the HIP algorithm. The residuals in global coordinates are shown as a function of iteration (left) and projected for 0,1,5 and 10 iterations (right).

procedure has been iterated 10 times using 200 000 simulated $Z^0 \rightarrow \mu^+\mu^-$ events. Figure 11 shows the differences between the true and estimated alignment parameters. The convergence is good, with RMS values of 7(23) μm for the $x, y(z)$ coordinates, respectively. The algorithm was also applied to a test beam setup¹⁰.

8. CONCLUSIONS

The CMS silicon tracker is a complex device, consisting of more than 15000 individual silicon sensors. The track reconstruction performance is very good, although the track reconstruction efficiency for low momentum charged hadrons is affected by the significant amount of tracker material.

Alignment of the tracker is a challenging task, and involves a laser alignment system as well as track-based alignment with the goal to determine the positions of all detector

modules with a precision of 10 μm , so that the intrinsic resolution of the silicon modules is not significantly degraded. To achieve this goal, CMS has implemented three different track-based alignment algorithms. Results from first alignment studies applying these algorithms to parts of the CMS tracker in simulation are very encouraging.

References

1. CMS Collaboration, “Physics Technical Design Report, Volume 1: Detector Performance and Software”, **CERN/LHCC 2006-001** (2006).
2. W. Adam et al., “Track reconstruction in the CMS tracker”, CMS Note **2006/041** (2006).
3. I. Belotelov et al., “Simulation of Misalignment Scenarios for CMS Tracking Devices”, CMS Note **2006/008** (2006).
4. P. Vanlaer et al., “Impact of CMS tracker misalignment on track and vertex reconstruction”, CMS Note **2006/029** (2006).

5. R. Fruehwirth et al., “A Kalman Filter for Track-based Alignment”, CMS Note **2006/022** (2006).
6. V. Blobel, “Millepede program description and code”, see <http://www.desy.de/~blobel/wwwmille.html>
7. P. Schleper et al., “Software Alignment of the CMS Tracker using Millepede-II”, CMS Note **2006/011** (2006).
8. V. Karimaki et al., “Sensor Alignment by Tracks”, CMS CR **2003/022** (2003), presented at CHEP 2003, La Jolla. [physics/0306034]
9. V. Karimaki et al., “The HIP Algorithm for track based alignment and its Application to the CMS pixel detector”, CMS Note **2006/018** (2006).
10. T. Lampen et al., “Alignment of the Cosmic Rack with the Hits and Impact Points Algorithm”, CMS Note **2006/006** (2006).